# Structural basis for selectivity of a small molecule, S1-binding, submicromolar inhibitor of urokinase-type plasminogen activator

Bradley A Katz, Richard Mackman, Christine Luong, Kesavan Radika, Arnold Martelli, Paul A Sprengeler, Jing Wang, Hedy Chan and Lance Wong

**Introduction:** Urokinase-type plasminogen activator (uPA) is a protease associated with tumor metastasis and invasion. Inhibitors of uPA may have potential as drugs for prostate, breast and other cancers. Therapeutically useful inhibitors must be selective for uPA and not appreciably inhibit the related, and structurally and functionally similar enzyme, tissue-type plasminogen activator (tPA), involved in the vital blood-clotting cascade.

**Results:** We produced mutagenically deglycosylated low molecular weight uPA and determined the crystal structure of its complex with 4-iodobenzo[*b*]thiophene-2-carboxamidine ($K_i = 0.21 \pm 0.02$ μM). To probe the structural determinants of the affinity and selectivity of this inhibitor for uPA we also determined the structures of its trypsin and thrombin complexes, of apo-trypsin, apo-thrombin and apo-factor Xa, and of uPA, trypsin and thrombin bound by compounds that are less effective uPA inhibitors, benzo[*b*]thiophene-2-carboxamidine, thieno[2,3-*b*]-pyridine-2-carboxamidine and benzamidine. The $K_i$ values of each inhibitor toward uPA, tPA, trypsin, tryptase, thrombin and factor Xa were determined and compared. One selectivity determinant of the benzo[*b*]thiophene-2-carboxamidines for uPA involves a hydrogen bond at the S1 site to $O\gamma_{Ser190}$ that is absent in the Ala190 proteases, tPA, thrombin and factor Xa. Other subtle differences in the architecture of the S1 site also influence inhibitor affinity and enzyme-bound structure.

**Conclusions:** Subtle structural differences in the S1 site of uPA compared with that of related proteases, which result in part from the presence of a serine residue at position 190, account for the selectivity of small thiophene-2-carboxamidines for uPA, and afford a framework for structure-based design of small, potent, selective uPA inhibitors.

Address: Axys Pharmaceutical Corporation, 385 Oyster Point Boulevard, Suite 3, South San Francisco, CA 94080, USA.

Correspondence: Bradley A Katz
Email: brad_katz@axyspharm.com

**Key words:** S1 structure, thrombin, tPA, trypsin, uPA

Received: **5 November 1999**
Revisions requested: **13 December 1999**
Revisions received: **14 January 2000**
Accepted: **11 February 2000**

Published: **23 March 2000**

**Chemistry & Biology** 2000, **7**:299–312

1074-5521/00/$ – see front matter


## Introduction

One of the basic hurdles in the development of enzyme inhibitors as drugs involves the achievement of selectivity toward the target enzyme and against its closely related counterparts. In serine proteases specificity of a physiological substrate is conferred by the combination of interactions at a series of sites, designated S3, S2, S1, S1′, S2′ and S3′, that bind successive peptide sidechains designated P3, P2 and P1 prior to the susceptible scissile peptide bond, and P1′, P2′ and P3′ after it [1]. Most inhibitors of a subset of trypsin-like serine proteases (which includes trypsin, tryptase, factor Xa, thrombin, urokinase-type plasminogen activator and tissue-type plasminogen activator) have a basic group that makes hydrogen-bonded salt bridges with the Asp189 carboxylate at the base of the S1 pocket, as for the arginine residue of a substrate. Interactions at the S1 site enable substrates or inhibitors to discriminate between the class of trypsin-like serine proteases with an aspartate residue at position 189 and other families such as chymotrypsin-like proteases, with a serine residue at position 189.

Selectivity of inhibitors for individual members within the family of trypsin-like serine proteases is often achieved through interactions of inhibitor groups at subsites such as S1′, S2 and S3, whose sequences and structures differ significantly from one member to the next [2–5]. Because of the high structural similarity in the S1 sites of the trypsin-like serine proteases with an aspartate residue at position 189, small-molecule inhibitors that achieve specificity for trypsin-like serine protease drug targets through interactions at this site alone merit close scrutiny. One such inhibitor is 4-iodobenzo[*b*]thiophene-2-carboxamidine, a lead compound from a series of over 90 4-substituted benzo[*b*]thiophene-2-carboxamidines reported in 1993 [6]. This compound stands out as a submicromolar competitive inhibitor of urokinase-type plasminogen activator (uPA), exhibiting selectivity for uPA and against plasmin, thrombin and tissue-type plasminogen activator (tPA).

Because of its involvement in tumor metastasis and invasion, uPA has emerged as a drug target for development of

therapeutics for prostate, breast and other cancers [7–11]. Therapeutic inhibitors of uPA should not appreciably inhibit the closely related enzymes (thrombin and tPA [12]), which are critical components of the blood-clotting pathway. Both uPA and tPA share the same primary physiological substrate (plasminogen) and inhibitor (plasminogen activator inhibitor), exhibit stringent specificity, and share similar sequences and three-dimensional structures [12,13]. Determination of the structural basis for the affinity and selectivity of 4-iodobenzo[*b*]thiophene-2-carboxamidine for uPA and against tPA and other related proteases is therefore expected to provide insight for structure-based design of selective, potent inhibitors of uPA and other trypsin-like protease targets.

To this end we determined the crystal structures of the uPA, trypsin and thrombin complexes of 4-iodobenzo[*b*]thiophene-2-carboxamidine, and the $K_i$ values of this inhibitor for trypsin-like serine protease drug targets and anti-targets: uPA, tPA, thrombin, factor Xa, tryptase and trypsin. Structural determinants of the binding of this scaffold were further examined by quantitating inhibition of each of the enzymes by structurally related analogs that are less effective inhibitors of uPA, benzo[*b*]thiophene-2-carboxamidine, thieno[2,3-*b*]pyridine-2-carboxamidine, and benzamidine, and by determining and comparing the structures of the uPA, trypsin and thrombin complexes. Finally, structures of inhibitor-free trypsin, factor Xa and thrombin were determined to delineate and compare features of the apo-enzymes, such as the ordered solvent structure at the S1 site that mediates the binding of the inhibitors investigated. The uPA–small-molecule structures of this study, involving fully reversible active site inhibitors, are among the first reported to date [11].

Although the S1 sites of uPA and tPA are structurally very similar, the identity of residue 190 is an important feature that distinguishes one from the other. uPA and tPA can be considered archetypes of two classes of trypsin-like serine proteases, those with a serine residue at position 190, such as uPA, trypsin and tryptase, and those with an alanine residue at position 190, such as tPA, thrombin and factor Xa. The differences in the architectures and hydrogen-bonding potentials of the S1 sites of these two protease families, as visualized in the structures of representative members determined here, both in the presence and absence of S1-bound inhibitors, provide a basis for selectivity development. Comparison within this set of structures of distinguishing features in the S1 site, such as its width and depth, its spatial relationship to the active site, and the nature and degree of its structural plasticity, yields clues for achieving inhibitor selectivity. The complementary structural and inhibition data of this study not only form a framework for the structure-based development of potent, selective uPA inhibitors, but also provide insight into the design of inhibitors that discriminate between these two large important classes of trypsin-like serine proteases.

## Results

### Affinity and selectivity of benzo[*b*]thiophene-2-carboxamidine analogs for uPA and for other trypsin-like serine proteases

We observed competitive inhibition by 4-iodobenzo-[*b*]thiophene-2-carboxamidine of each member of a panel of trypsin-like serine proteases comprising uPA, trypsin, tryptase, tPA, thrombin and factor Xa. The inhibition constant ($K_i$ value) determined here for uPA at pH 7.4 is $0.21 \pm 0.02$ μM (Table 1), compared with $0.53 \pm 0.07$ μM determined at pH 7.5 by Towle *et al.* [6]. The $K_i$ value for tPA, an anti-target closely related structurally and functionally to uPA, is $16.8 \pm 0.4$ μM, yielding a selectivity ratio for tPA versus uPA of 80. Also listed in Table 1 are the $K_i$ values for benzo[*b*]thiophene-2-carboxamidine, thieno[2,3-*b*]pyridine-2-carboxamidine and benzamidine toward each protease. Our determined selectivity ratios of 4-iodobenzo[*b*]thiophene-2-carboxamidine toward uPA

**Table 1**

**Inhibition constants of amidine inhibitors toward selected trypsin-like serine proteases.**

| | Ser190 proteases | | | Ala190 proteases | | |
|---|---|---|---|---|---|---|
| Inhibitor | uPA | Trypsin | Tryptase | tPA | Thrombin | Factor Xa |
| APC-6860* | **0.21 ± 0.02** | **0.44 ± 0.1** | 1.5 ± 0.1 | 16.8 ± 0.4 | **20 ± 2** | 30 ± 2 |
| APC-7377† | 2.3 ± 0.2 | **1.0 ± 0.1** | 9.9 ± 0.8 | 15 ± 1 | 58 ± 5 | 21 ± 2 |
| APC-7538‡ | **63 ± 5** | **80 ± 5** | 34 ± 2 | 1800 ± 100 | 1600 ± 200 | 360 ± 110 |
| Benzamidine | **97 ± 9** | **21 ± 2** | 20 ± 2 | **750 ± 70** | **320 ± 25** | 110 ± 20 |
| None | | **apo** | | | **apo** | **apo** |

All $K_i$ values in μM. Bold values denote structures determined here or elsewhere (tPA–benzamidine) [12]. *4-Iodobenzo[*b*]thiophene-2-carboxamidine. Competitive inhibition was demonstrated and $K_i$ values determined rigorously for each enzyme by varying both the substrate and the inhibitor concentrations. For the other compounds, $K_i$ values were determined at one substrate concentration (per enzyme) set near the determined $K_m$ value (see text). †Benzo[*b*]thiophene-2-carboxamidine. ‡Thieno[2,3-*b*]pyridine-2-carboxamidine.

and against plasmin (15, data not shown), thrombin and tPA (95 and 80, respectively) are significantly less than the corresponding values in the study of Towle *et al.* (1100, > 780 and 330, respectively) [6].

4-Iodobenzo[*b*]thiophene-2-carboxamidine is a significantly better inhibitor of the Ser190 proteases listed in Table 1, uPA, trypsin and tryptase ($K_i$ = 0.2–1.5 μM), than the Ala190 counterparts, tPA, thrombin and factor Xa ($K_i$ = 17–30 μM). In general, the other inhibitors in Table 1 show a similar trend. Factors other than the identity of residue 190 can also influence inhibitor potency, however. For example, benzo[*b*]thiophene-2-carboxamidine is a 9.9-fold better inhibitor of trypsin (1.0 μM) than of tryptase (9.9 μM), both of which have a serine residue at position 190. In addition, uPA (with Ser190) is inhibited by benzamidine ($K_i$ = 97 μM) about as weakly as is factor Xa (with Ala190; $K_i$ = 110 μM).

Benzo[*b*]thiophene-2-carboxamidine is a poorer inhibitor of uPA and tryptase than the 4-iodo analog, by factors of 11 and 6.6, respectively (Table 1). The 4-iodo substituent has little effect on the $K_i$ values of the other proteases. Introduction of a nitrogen into the six-membered ring of benzo[*b*]thiophene, in thieno[2,3-*b*]pyridine-2-carboxamidine, leads to a decrease in affinity toward all of the enzymes that ranges from as little as 3.4-fold for tryptase to as much as 120-fold for tPA.

### Benzo[*b*]thiophene-2-carboxamidines bound to uPA make a hydrogen bond with Ser190 that is absent in Ala190 counterparts

Figure 1a shows the structure of uPA–4-iodobenzo[*b*]thiophene-2-carboxamidine, pH 6.5, superimposed on the $(2|F_o|-|F_c|)$, $\alpha_c$ map. The inhibitor amidine lies at the bottom of the S1 site, making two hydrogen-bonded salt bridges with the carboxylate of Asp189. One amidine nitrogen also donates a hydrogen bond to the carbonyl oxygen of Gly219. The remaining amidine hydrogen (H1) is donated in a multi-centered hydrogen-bonding interaction to $O\gamma_{Ser190}$ and to an ordered water (water1). The hydrogen-bond parameters at the S1 site for this and other structures are listed in Table 2.

In Figure 1b the structure of uPA–4-iodobenzo[*b*]thiophene-2-carboxamidine is superimposed on the corresponding thrombin complex. As in the uPA and trypsin complexes, a water co-bound at the S1 site mediates inhibitor binding. The $N1_{inhibitor}$–$O\gamma_{Ser190}$ and water1–$O\gamma_{Ser190}$ hydrogen bonds present in the uPA and trypsin complexes are absent in the thrombin complex, however, because residue 190 is an alanine in thrombin. One of the components (N1–$O\gamma_{Ser190}$) of the multi-centered enzyme–inhibitor hydrogen bond in the uPA and trypsin complexes is therefore absent in the thrombin complex. The remaining component (N1–water1) is shorter in the thrombin complex (2.9 Å at pH 7.3) than in the uPA

**Figure 1**

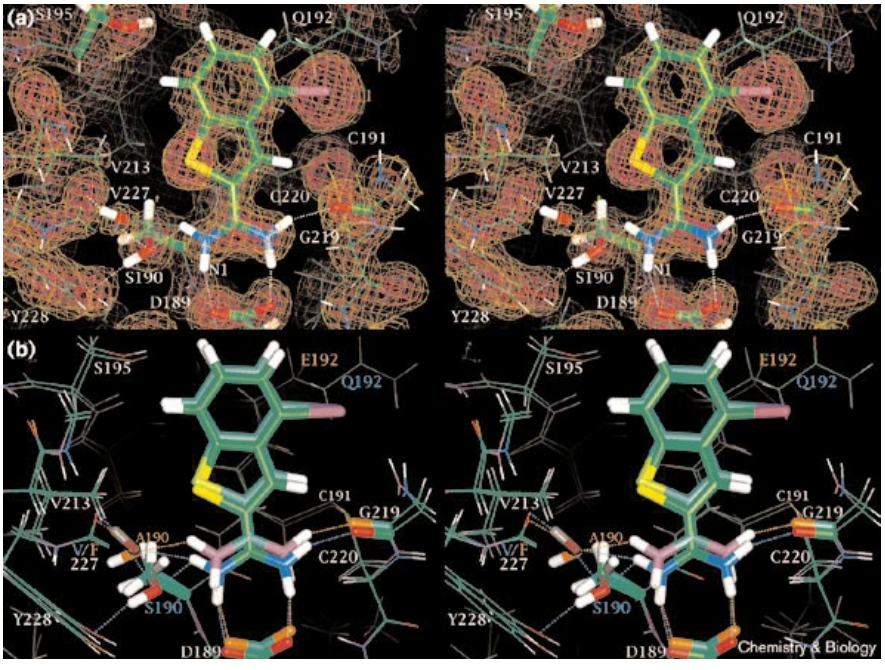


**(a)** Superposition of the structure of uPA–4-iodobenzo[*b*]thiophene-2-carboxamidine, pH 6.5, onto the $(2|F_o|-|F_c|)$, $\alpha_c$ map (1.75 Å resolution). In this and other density figures contours are at 1.0 σ (light orange), 2.4 σ (red) and 3.8 σ (pink). The shorter (N1–$O\gamma_{Ser190}$) component of the 3-centered hydrogen bond is yellow, the longer (N1–water1) component is cyan. **(b)** Superposition of the thrombin– and uPA–4-iodobenzo[*b*]thiophene-2-carboxamidine complexes. In this and other figures comparing uPA with another structure, carbon, oxygen and nitrogen atoms are green, red and blue, respectively, for uPA, and light green, orange and purple, respectively, for the other complex. Residues common to both structures are labeled in white, those unique to uPA in light blue and those unique to the other enzyme in orange. Hydrogen bonds at S1 are light blue for uPA, and orange for the other enzyme. The long (3.21 Å) N1–water hydrogen bond in the uPA complex is cyan. The directionalities of the hydrogen bonds involving $O\gamma_{Ser190}$ and $O\eta_{Tyr228}$ in the uPA complex can be inferred from the following: a well-ordered water donates one proton to $O_{Ala183}$, and the other to $O\delta1_{Asp189}$ (data not shown). The other hydrogen bond to this water, involving $O\eta_{Tyr228}$, is therefore donated by $O\eta_{Tyr228}$, the $H\eta_{Try228}$ proton lying in the aromatic plane. $O\eta_{Tyr228}$ therefore accepts the hydrogen bond from $O\gamma_{Ser190}$.

**Table 2**

**Hydrogen bond lengths and angles, inhibitor dihedrals, and temperature factor of co-bound water at the S1 site.**

**(a) uPA, tPA, trypsin and thrombin complexes of benzo[*b*]thiophene-2-carboxamidine analogs and of benzamidine.**

| | pH | N2–$O\delta2_{Asp189}$ | N2–$O_{Gly219}$ | N1–$O\delta1_{Asp189}$ | N1–$O\gamma_{Ser190}$ | N1–H1–$O\gamma_{Ser190}$ | Inhibitor dihedral |
|---|---|---|---|---|---|---|---|
| uPA–APC-6860* | 5.5 | 2.85(02) | 2.77(02) | 2.83(03) | 2.72(05) | 121(2) | 11(3) |
| Thrombin–APC-6860 | 7.3 | 2.81 | 2.62 | 3.13 | | | –1 |
| Trypsin–APC-6860 | 8.2 | 2.87 | 2.76 | 3.09 | 2.92 | 111 | 5 |
| Trypsin–APC-6860 | 5.5 | 2.85 | 2.66 | 2.81 | 2.77 | 129 | 18 |
| Trypsin–APC-7377† | 8.2 | 2.80 | 2.72 | 2.85 | 2.91 | 127 | 4 |
| uPA–APC-7538‡ | 5.5 | 2.83 | 2.79 | 2.80 | 2.63 | 116 | 9, 2‡ |
| Trypsin–APC-7538 | 5.5 | 2.80 | 2.73 | 2.83 | 2.84 | 124 | –11, –11‡ |
| Trypsin–APC-7538 | 8.2 | 2.90 | 2.76 | 2.89 | 2.87 | 119 | –11, –9‡ |
| Trypsin–benzamidine§ | 7.5 | 2.93(05) | 2.68(09) | 2.90(04) | 2.88(11) | 120(2) | –20(2) |
| Thrombin–benzamidine | 7.3 | 2.76 | 2.59 | 2.95 | | | –7 |
| uPA–benzamidine | 5.5 | 2.94 | 2.74 | 2.88 | 2.52 | 115 | 5 |
| tPA–benzamidine# | 7.5 | 3.00 | 2.82 | 2.96 | | | –3 |

**(b) complexes plus inhibitor-free trypsin, thrombin, and factor Xa.**

| | pH | N1–$OH_2$ | N1–H1–$OH_2$ | $O\gamma_{Ser190}$–$OH_2$ | $O_{Val/Phe/Ile227}$–$OH_2$ | $O_{Trp215}$–$OH_2$ | B ($H_2O$) |
|---|---|---|---|---|---|---|---|
| uPA–APC-6860 | 5.5 | 3.21(04) | 130(8) | 3.01(11) | 3.18(13) | 3.42(02) | 29(1) |
| Thrombin–APC-6860 | 7.3 | 2.91 | 130 | | 3.07 | 3.60 | 19 |
| Trypsin–APC-6860 | 8.2 | 3.12 | 142 | 3.16 | 2.98 | 3.39 | 25 |
| Trypsin–APC-6860 | 5.5 | 3.47 | 118 | 3.18 | 2.89 | 3.32 | 24 |
| Trypsin–APC-7377 | 8.2 | 3.15 | 119 | 2.91 | 3.05 | 3.20 | 24 |
| uPA–APC-7538 | 5.5 | 3.26 | 130 | 3.19 | 3.11 | 3.20 | 20 |
| Trypsin–APC-7538 | 5.5 | 3.16 | 128 | 3.12 | 2.98 | 3.08 | 18 |
| Trypsin–APC-7538 | 8.2 | 3.07 | 131 | 3.21 | 2.87 | 3.01 | 20 |
| Trypsin–benzamidine | 7.5 | 3.04(06) | 142(6) | 3.14(06) | 2.87(05) | 3.06(06) | 18(2) |
| Thrombin–benzamidine | 7.3 | 2.73 | 150 | | 3.25 | 3.29 | 16 |
| uPA–benzamidine | 5.5 | 2.96 | 136 | 2.84 | 3.26 | 3.41 | 19 |
| tPA–benzamidine | 7.5 | 3.06 | 154 | | 2.83 | 3.36 | 26 |
| apo-trypsin | 5.0 | | | 2.70 | 3.33 | 3.22 | 29 |
| apo-trypsin | 7.7 | | | 3.00 | 3.02 | 3.12 | 29 |
| apo-thrombin | 7.8 | | | | 3.06 | 3.36 | 34 |
| apo-factor Xa | 7.5 | | | | 2.76 | 3.20 | 41 |

Distances are in Å, temperature factors (B-values) in Å$^2$, and the ring-amidine dihedral in degrees. Standard deviations are in parentheses. *APC-6860, 4-Iodobenzo[*b*]thiophene-2-carboxamidine. †APC-7377, Benzo[*b*]thiophene-2-carboxamidine. ‡APC-7538, Thieno-[2,3-*b*]pyridine-2-carboxamidine. The dihedral angles are for conformations 1 and 2 (see text) §Ten structures (pH 7.00 to 8.25) of resolutions higher than 1.5 Å. #1rtf [12].

complex (3.2 Å at pH 6.6) or than in the trypsin complex (3.1 Å at pH 8.2, or 3.5 Å at pH 5.5). The N1–H1–$O_{water1}$ angle of this interaction is nonoptimal (~130°) and similar in all complexes (Table 2).

The decrease in the N1–water1 hydrogen bond length in thrombin–4-iodobenzo[*b*]thiophene-2-carboxamidine from that in the corresponding uPA complex is accomplished by a rotation of the inhibitor amidine group by 12° around the thiophene–amidine bond; in the thrombin complex the amidine is virtually coplanar with the thiophene (dihedral = –1°). The change in the inhibitor geometry to planarity in the thrombin complex is associated with an increase in the N1–$O\delta1_{Asp189}$ hydrogen bond from 2.8 Å in the uPA complex to 3.1 Å in the thrombin complex.

### Interactions and environment of the iodo group in 4-iodobenzo[*b*]thiophene-2-carboxamidine complexes

The density corresponding to the iodo group is very strong (23 σ in the uPA and trypsin complexes). The iodo group occupies a cavity, making van der Waals contacts with $C\delta_{Gln192}$ (3.7 Å), $S\gamma_{Cys220}$ (4.2 Å), $O_{Gly216}$ (3.9 Å), and

$N_{Gly219}$ (4.3 Å) in the uPA complex, and similar contacts in the trypsin and thrombin complexes. The structure of trypsin–benzo[*b*]thiophene-2-carboxamidine is virtually identical to that of the 4-iodo analog complex.

### Variability in the structures of bound amidine inhibitors

Comparison of the structures of the inhibitor complexes of uPA, tPA, trypsin and thrombin denoted by the bold entries in Table 1 reveals a remarkable diversity in the binding of such small inhibitors. The complexes can be divided roughly into two groups based on the orientations of the aromatic planes of the bound inhibitors. The inhibitors in the first set are rotated by ~20° from those in the second set around their long symmetry axis. Consequently the amidines in the first set are rotated around the amidine-aromatic bond by ~–20° from those in the second set in order to maintain hydrogen-bonding interactions at S1. The first set includes trypsin–, thrombin– and uPA–4-iodobenzo[*b*]thiophene-2-carboxamidine, uPA–thieno[2,3-*b*]pyridine-2-carboxamidine, and uPA– and tPA–benzamidine; the second set trypsin– and thrombin–-benzamidine, and trypsin–thieno[2,3-*b*]pyridine-carboxamidine. The aromatic amidine dihedrals for the bound inhibitors range from –20° to +18° (Table 2).

### Diversity in the S1 site architectures of the trypsin-like serine proteases complexes

Differences in the bound structure of benzamidine or of other small amidine inhibitors among the trypsin-like protease complexes reflect subtle but significant changes in the corresponding S1 site architectures. In uPA–benzamidine there are shifts (of ~0.5 Å) in the position of $O\gamma_{Ser190}$, $O\eta_{Tyr228}$, and water1 from the respective locations in trypsin–benzamidine (Figure 2a, Table 3a). In trypsin–benzamidine (and in many other trypsin–amidine complexes) water1 makes four hydrogen bonds. In the hydrogen-bonding scheme of Figure 2a, water1 accepts hydrogen bonds from $O\gamma_{Ser190}$, (3.14 ± 0.06 Å) and from $N1_{benzamidine}$ (3.04 ± 0.06 Å), and donates hydrogen bonds to $O_{Trp215}$ (3.06 ± 0.06 Å) and to $O_{Val227}$ (2.87 ± 0.05 Å;

**Figure 2**

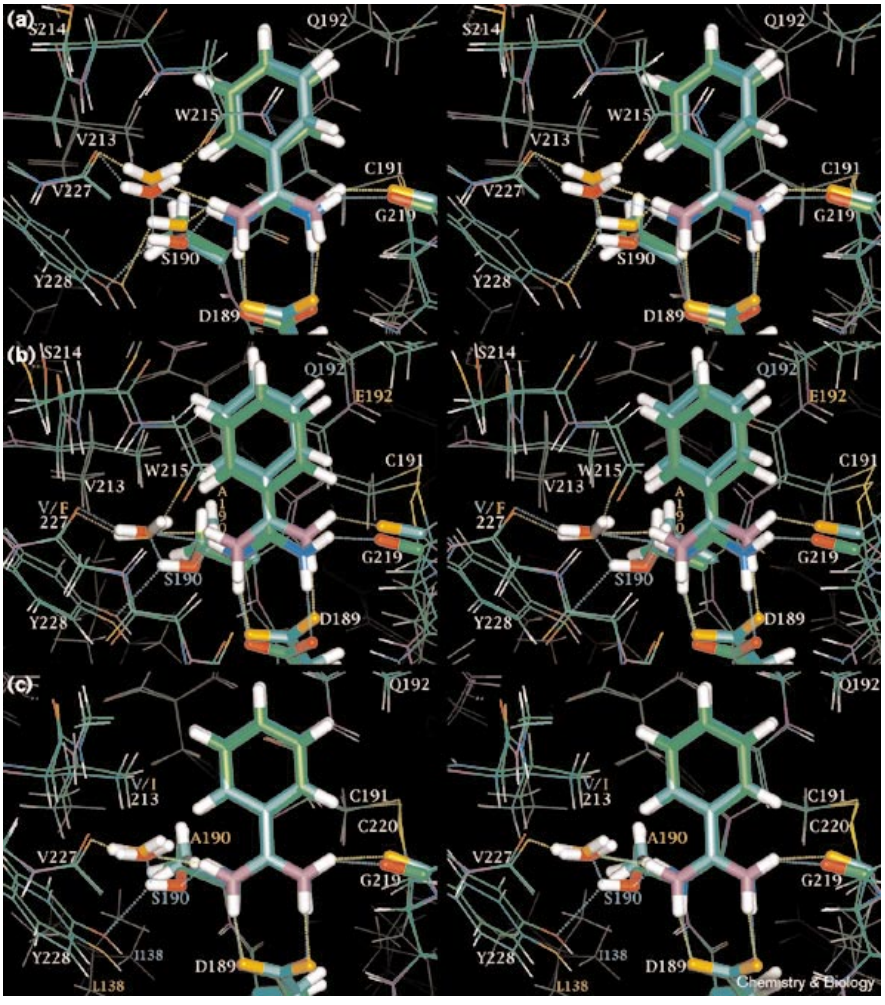


**(a)** Superposition of the structures of trypsin–benzamidine, pH 7.5, at 1.21 Å resolution, and uPA–benzamidine, pH 6.5, at 1.85 Å resolution. Hydrogen bonds for the trypsin and uPA complexes are yellow and light blue, respectively. The long water1–$O_{Val227}$ interaction in uPA–benzamidine (3.26 Å) is darker cyan. In addition to any hydrogen bonds accepted from water1, the carbonyl oxygens of residues 215 and 227 also accept β-sheet hydrogen bonds, with better angular components, from the peptide nitrogens of residues 227 and 215, respectively, in these and other structures. In the hydrogen-bonding scheme shown, $O\gamma_{Ser190}$ donates a multi-centered hydrogen bond to water1 and to $O\eta_{Tyr228}$. Other orientations of water1 and alternate hydrogen bonding $O\gamma_{Ser190}$–water1 directionalities are possible, especially in cases where hydrogen bonds to the carbonyl oxygens of residues 215 and/or 227 are absent, as in Figure 1. **(b)** Superposition of thrombin–benzamidine onto uPA–benzamidine using corresponding mainchain atoms from residues 43–45, 53, 54, 191–197, 212–221 and 227–229 yields a 0.25 Å rms deviation between these two sets of atoms. **(c)** Superposition of tPA–benzamidine (1rtf [12]) onto uPA–benzamidine.

Table 2). In uPA–benzamidine, however, the latter hydrogen bonds are absent (water1–$O_{Trp215}$ = 3.4 Å, water1–$O_{Val227}$ = 3.3 Å). Their absence is associated with shorter N1–$O\gamma_{Ser190}$ and water1–$O\gamma_{Ser190}$ hydrogen bonds (2.5 Å and 2.8 Å) than in the other trypsin and uPA complexes (Table 2). The difference in hydrogen-bonding interactions involving water1 between uPA– and trypsin–benzamidine is not seen between uPA– and trypsin–4-iodobenzo[*b*]thiophene-2-carboxamidine. In both of the latter complexes water1 makes hydrogen bonds with $O\gamma_{Ser190}$, N1 and $O_{Val/Phe227}$, but not with $O_{Trp215}$ (Table 2).

Table 3a lists the overall root mean square deviations (rmsds) and selected individual atomic differences between the superimposed inhibitor-binding sites of pairs of benzamidine complexes of trypsin, uPA, thrombin and tPA, along with the percent of sequence identity between the catalytic domains (heavy chains) of each pair or between their structural cores. There is a rough correlation between overall (and core) sequence similarity and similarity in the S1 site architecture. The two most structurally similar S1 sites (rmsd 0.29 Å) belong to the pair of proteases with the highest overall sequence identity, uPA/tPA (45.6%). The largest structural variations (rmsd 0.41 Å) occur for the pair with the second lowest overall sequence identity, thrombin/tPA (31.5%, Table 3a).

In each of the structures of this study the S1, S1′ and active-site residues Cys42, His57, Asp189, Ser195 and Tyr228, common to uPA, tPA, trypsin, tryptase, thrombin, and factor Xa, are well determined by density and have low temperature factors (Table S1b in the Supplementary material section). The relative locations of selected atoms of these residues vary significantly between complexes, however, by as much as 1 Å (Table 3a), irrespective of the identity of residue 190. The differences between proteases in the sidechain position and conformation of Tyr228 can be seen in Figure 2a–c for the comparisons of the benzamidine complexes of uPA, trypsin, thrombin and tPA. These types of subtle differences define a unique set of S1 site dimensions (Table S1a) that distinguish one protease from another, providing a fingerprint of each particular protease.

Table 3c also summarizes some control comparisons. Overall, there are minor differences between the benzamidine-binding sites of trypsin crystal forms $P3_121$ and $P2_12_12_1$, although some moderate and highly reproducible differences do occur. Because neighboring protein molecules do not directly contact any of the bound inhibitors or inhibitor-binding sites in either crystal form, the differences must reflect indirect, and relatively long-range effects of crystal packing. Identical structures independently determined in the same crystal form exhibit negligible structural differences (rmsd 0.05 Å; Table 3c), and emphasize the accuracy of the structural determinations.

A dramatic increase in the depth of the S1 site of uPA compared with that of thrombin is apparent in the comparison of the structures of uPA– and thrombin–benzamidine (Figure 2b). Bound benzamidine is shifted by 0.5 Å, and the Asp189 sidechain is correspondingly shifted by ~0.6 Å (Table 3a). The relative positions of the bound inhibitors and of the Asp189 sidechain are significantly different in many of the comparisons that involve a common bound inhibitor. The largest differences occur between uPA and thrombin. By contrast, the structures of the S1 sites of uPA and tPA are highly similar (Figure 3c) and have the lowest overall rms deviations from one another, 0.29 Å (Table 3a). Benzamidine binds in a similar relative position and orientation, and with a similar planarity to these two related proteases (Figure 3c). The high similarity of the uPA– and tPA–benzamidine complexes underscores the effect of residue 190 on inhibitor potency. The most obvious difference between the complexes, the absence of the Ser190 sidechain and of the associated hydrogen bond to benzamidine in the tPA complex, is strongly implicated in the 7.7-fold decrease in potency.

### Discrete conformational disorder in thieno[2,3-*b*]pyridine-2-carboxamidine bound to uPA and trypsin

In uPA–thieno[2,3-*b*]pyridine-2-carboxamidine, pH 6.5, and in the corresponding trypsin complex, pH 5.5 and 8.2, the inhibitor is discretely disordered between two conformations involving a 180° rotation of the thieno[2,3-*b*]pyridine moiety about the amidine–thiophene bond. The disorder was discovered and verified as described in the Supplementary material section. Figure 3a shows the structure and ($2|F_o|-|F_c|$), $\alpha_c$ map for uPA–thieno[2,3-*b*]-pyridine-2-carboxamidine, pH 6.5. In the first conformation the sulfur is in a favorable location, as in bound benzo[*b*]thiophene-2-carboxamidines. Water1 is shifted, by 0.5 Å, from its position in uPA–4-iodobenzo[*b*]thiophene-2-carboxamidine, donating a shorter hydrogen bond to the thiophene sulfur (3.0 Å versus 3.3 Å), and coming into hydrogen-bonding range of $O_{Trp215}$ (3.2 Å versus 3.4 Å). In the first conformation of bound thieno[2,3-*b*]pyridine-2-carboxamidine, the inhibitor nitrogen is not in a favorable location, buried without hydrogen bonds, 3.6 Å from $O\gamma_{Ser195}$. In the second conformation, the nitrogen is in a more favorable location, exposed to solvent but the sulfur is in a less favorable location, making a close S–$O_{Gly219}$ contact (3.3 Å; Figure 3a).

In trypsin–thieno[2,3-*b*]pyridine-2-carboxamidine, the nitrogen of the second conformer does make a hydrogen bond (3.1 Å) with $O\gamma_{Ser195}$, because the bound inhibitor is 0.5 Å higher in the S1 site than in the uPA complex (Figure 3b). At pH 8.2 it can be inferred that $O\gamma_{Ser195}$ is the hydrogen-bond donor to both $N\varepsilon2_{His57}$ and to the inhibitor nitrogen. Consequently there is a deficit in hydrogen-bonding interactions involving the buried inhibitor nitrogen, $O\gamma_{Ser195}$ and $N\varepsilon2_{His57}$. At pH 5.5 a

**Table 3**

**Comparison of structures of benzamidine complexes of trypsin, uPA, thrombin, and tPA, and of apo-trypsin and apo-thrombin.**

| | Sub-site | S1 | | | | | | | | | |
|---|---|---|---|---|---|---|---|---|---|---|---|
| | Residue | Ser/Ala190 | Asp189 | | | Tyr228 | | Gly219 | Inhibitor | | $H_2O(1)$ |
| | Atom | Oγ | Cβ | Oδ1 | Oδ2 | Oη | Cε2 | O | N1 | N2 | O |
| **(a)** | Thrombin/uPA | | **0.52** | 0.33 | **0.75** | 0.22 | 0.23 | **0.59** | 0.41 | **0.61** | 0.09 |
| | Thrombin/tPA | | **0.64** | 0.18 | **0.61** | 0.31 | 0.17 | 0.26 | 0.21 | 0.31 | 0.29 |
| | Trypsin/thrombin | | **0.50** | 0.22 | **0.55** | **0.82** | **0.67** | 0.35 | 0.21 | 0.22 | **0.65** |
| | Trypsin/uPA | **0.52** | 0.22 | 0.30 | 0.38 | **0.52** | **0.49** | 0.20 | **0.50** | 0.31 | **0.45** |
| | Trypsin/tPA | | **0.65** | 0.16 | 0.21 | **0.77** | **0.58** | 0.25 | 0.25 | 0.28 | **0.46** |
| | uPA/tPA | | 0.43 | 0.25 | 0.29 | **0.54** | 0.37 | 0.37 | **0.55** | 0.10 | 0.30 |
| **(b)** | Trypsin/apo-trypsin | **0.57** | 0.44 | 0.14 | 0.29 | 0.15 | 0.16 | 0.16 | | | 0.19 |
| | Thrmb/apo-thrombin | | 0.14 | 0.37 | 0.42 | 0.20 | 0.15 | 0.34 | | | **0.55** |
| **(c)** | Trypsin*, $P3_121/P2_12_12_1$ | 0.14 | 0.11 | 0.19 | 0.16 | 0.12 | 0.10 | 0.19 | 0.37 | 0.33 | 0.22 |
| | Trypsin†, $P3_121/P3_121$ | 0.12 | 0.05 | 0.05 | 0.05 | 0.05 | 0.02 | 0.10 | 0.05 | 0.06 | 0.05 |
| | Trypsin‡, $+SO_4^{-2}/-SO_4^{-2}$ | 0.09 | 0.05 | 0.05 | 0.04 | 0.03 | 0.06 | 0.05 | 0.05 | 0.04 | 0.04 |

| | Sub-site | S1′ | Active site | | | | | | | Sequence | |
|---|---|---|---|---|---|---|---|---|---|---|---|
| | Residue | Cys42 | Ser195 | | His57 | Gln/Glu192 | Residues withheld | | | identity | |
| | Atom | N | Oγ | Cβ | Nε2 | Cα | from superposition§ | rmsi§ | rmsf§ | Overall | Core# |
| **(a)** | Thrombin/uPA | 0.40 | **1.07** | 0.24 | **1.07** | **0.56** | 42, 57–58, 189–190, 192–193 | 0.36 | 0.25 | 27.8 | 44.1 |
| | Thrombin/tPA | **0.74** | **0.99** | **0.48** | **0.54** | **0.65** | 42, 44–45, 57–58, 190, 192¶ | 0.41 | 0.33 | 31.5 | 47.5 |
| | Trypsin/thrombin | 0.41 | **0.59** | **0.46** | 0.39 | **0.65** | 53, 58, 189–190, 192 | 0.37 | 0.33 | 34.4 | 49.2 |
| | Trypsin/uPA | **0.76** | **0.52** | 0.39 | **0.89** | 0.38 | 42, 57 | 0.35 | 0.28 | 35.2 | 48.3 |
| | Trypsin/tPA | **0.72** | **0.59** | **0.64** | 0.30 | 0.31 | 42, 53, 190, 193, 195 | 0.38 | 0.38 | 36.9 | 52.5 |
| | uPA/tPA | 0.26 | 0.23 | 0.28 | **0.57** | 0.06 | 43–45, 53–54 | 0.29 | 0.25 | 45.6 | 61.9 |
| **(b)** | Trypsin/apo-trypsin | 0.09 | **0.54** | 0.20 | 0.32 | 0.29 | 190–192 | 0.14 | 0.12 | | |
| | Thrmb/apo-thrombin | 0.17 | **0.56** | 0.25 | 0.12 | **0.61** | 191–192 | 0.27 | 0.25 | | |
| **(c)** | Trypsin*, $P3_121/P2_12_12_1$ | 0.05 | 0.32 | 0.14 | 0.35 | **0.50** | 192 | 0.13 | 0.12 | | |
| | Trypsin†, $P3_121/P3_121$ | 0.06 | 0.14 | 0.12 | 0.12 | 0.02 | | 0.05 | 0.05 | | |
| | Trypsin‡, $+SO_4^{-2}/-SO_4^{-2}$ | 0.06 | 0.37 | 0.22 | 0.17 | 0.02 | | 0.05 | 0.05 | | |

Differences are in Å, and sequence identity is in %. Differences greater than 0.45 Å are in bold. In **(a)** and **(b)** all trypsin–benzamidine comparisons involve $P3_121$ trypsin–benzamidine-sulfate, pH 7.50, 1.21 Å resolution. Sulfate and citrate are co-bound at the active sites of tPA– and uPA–benzamidine, respectively. *Trypsin–benzamidine, both forms at pH 8.2, with no co-bound sulfate. The $P2_12_12_1$ form is the 'small cell' form (a = 54.8 Å, b = 58.7 Å, c = 67.6 Å). †Trypsin–benzamidine, pH 7.0 and 7.5, sulfate co-bound at each pH. ‡Trypsin–benzamidine, both in form $P3_121$, one at pH 7.7, with co-bound sulfate, and the other at pH 8.25 (and otherwise identical soaking conditions) without co-bound sulfate. §Mainchain atoms of residues 42–45, 53–54, 57–58, 189–197, 212–221 and 227–229 were used for initial superpositions of S1, S1′ and active sites, yielding overall initial rmsd, rmsi. Residues with significant differences in mainchain positions between corresponding atom pairs were withheld from final superpositions (for Figures and final comparisons), yielding 'rmsf'. #Core residues are 26–34, 41–58, 65–71, 81–91, 102–108, 117–124, 135–144, 154–164, 180–183, 189–200, 210–215 and 226–240. ¶Also excluded were residues 193, 195, 213 and 216–219.

sulfate is co-bound with partial occupancy (60%) at the active site, receiving hydrogen bonds from $N\varepsilon2_{His57}$, $O\gamma_{Ser195}$, and $N_{Gly193}$, as in trypsin–benzamidine-sulfate, or –BABIM-sulfate [14] (Figure 3b). The Hγ proton of Ser195 is disordered, donating partial hydrogen bonds to two of the oxygens of the co-bound sulfate in one location, and donating a hydrogen bond to the nitrogen of conformer 2 of the inhibitor in the other location (Figure 3b). (The $pK_a$ of the thieno[2,3-*b*]pyridine nitrogen is estimated to be ~4.9 [15].) The aromatic planes of the inhibitor conformers in uPA–thieno[2,3-*b*]pyridine-2-carboxamidine are rotated ~17° from those in the trypsin–thieno[2,3-*b*]pyridine-2-carboxamidine (Figure 3b), but are oriented similarly to those in uPA– and trypsin–4-iodobenzo[*b*]thiophene-2-carboxamidine. No binding of thieno[2,3-*b*]pyridine-2-carboxamidine to thrombin was observed crystallographically at an inhibitor concentration of 1 mM.

**Figure 3**

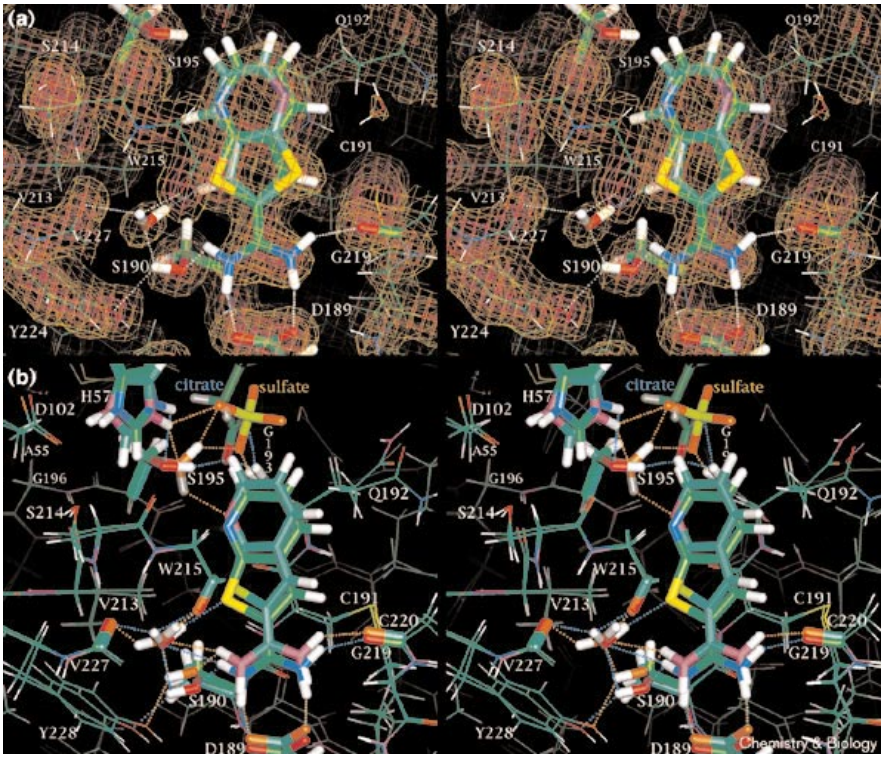


**(a)** Structure of uPA–thieno[2,3-*b*]pyridine-2-carboxamidine, pH 6.5, at 1.65 Å resolution, on the $(2|F_o|-|F_c|)$, $\alpha_c$ map. The occupancies of conformation 1 (with green carbons) and 2 (light green carbons) are 66% and 34%, respectively. In the trypsin complex the corresponding occupancies are 54% and 46% at pH 5.5, and 31% and 69% at pH 8.2. **(b)** Superposition of uPA– and trypsin–thieno[2,3-*b*]pyridine-2-carboxamidine, pH 5.5. For clarity only the first conformation of the bound inhibitors is shown. In each complex the aromatic rings of the two bound conformations of the inhibitors lie in the same plane as one another (see Figure 4a). The two locations of the Hγ proton of Ser195 for the trypsin complex are shown.

### Structural comparison of inhibitor complexes with corresponding inhibitor-free enzymes

The B factors of protein groups making hydrogen bonds with trypsin ($O\delta1,2_{Asp189}$, $O\gamma_{Ser190}$ and $O_{Gly219}$,) decrease significantly upon inhibitor binding (Table S1b), and the $O\gamma_{Ser190}$ atom undergoes a large shift, 0.5 Å in trypsin–benzamidine (Table 3b). Binding of benzamidine to thrombin decreases the B factors of $N\varepsilon2_{His57}$, $O\delta1,2_{Asp189}$ and $C\beta_{Ala190}$ (Table S1b). Binding of inhibitors to thrombin incurs greater and more extensive structural changes than does binding of the same inhibitors to trypsin. The rms deviations between the superimposed inhibitor-binding sites of thrombin–benzamidine and apo-thrombin is 0.27 Å, compared with 0.14 Å for trypsin–benzamidine/apo-trypsin (Table 3b). Binding of benzamidine induces a major contraction of the S1 site of thrombin, by 0.8 Å, along the $C\alpha_{Glu192}$–$C\alpha_{Trp215}$ vector, compared with only 0.2 Å for trypsin (Table S1a). In thrombin the contraction is reflected in a 0.6 Å change in the position of $C\alpha_{Glu192}$ (Table 3b).

The water (water1) that mediates inhibitor binding at S1 in the complexes is bound in a similar location in the structures of apo-trypsin (Figure 4a), apo-thrombin (Figure 4b) and apo-factor Xa. In apo-trypsin water1 makes hydrogen bonds with $O\gamma_{Ser190}$, $O_{Val227}$, $O_{Trp215}$, as in trypsin–benzamidine, and trypsin–thieno[2,3-*b*]pyridine-2-carboxamidine, and makes a fourth hydrogen bond with another ordered water (Figure 4a). Although there is a moderate increase in mobility of this water (29 $Å^2$) compared with that in the complexes (B = 18–25 $Å^2$), it is well ordered in apo-trypsin in terms of both location and orientation.

In thrombin, water1 undergoes a more pronounced decrease in B factor, from 16–19 $Å^2$ to 34 $Å^2$, upon inhibitor binding. In apo-thrombin, water1 makes only one hydrogen bond with the protein (with $O_{Phe227}$) and one with another water (B = 47 $A^2$; Figure 4b). In apo-factor Xa water1 is in a similar environment, and not well ordered (B = 41 $Å^2$). There are more possible orientations of water1 in the Ala190 apo-proteases, thrombin and factor Xa because water1 lacks the hydrogen-bonding interactions provided by $O\gamma_{Ser190}$ and $O_{Trp215}$ in apo-trypsin. Upon inhibitor binding to the Ala190 proteases, acceptance by water1 of the hydrogen bond donated by N1 of the inhibitor amidine causes an increase in the positional and/or rotational order of water1 (reflected by a large decrease in B factor) that represents an unfavorable entropy component to inhibitor binding.

### Comparison of the uPA structures of this study with that published previously

Some of the differences between the uPA structures of this study (space group C2, resolutions up to 1.65 Å) and the previously published structure (space group R3, 2.5 Å resolution, 1lmw [13] in the Brookhaven Database [16]) occur

on the surface and are due to differences in crystal packing. Other significant differences, however, reflect the higher resolution and level of refinement of these new uPA structures (see Table 4 and Table S2 in the Supplementary material section for refinement statistics). For example, in the R3 structure the loop comprising residues 185A–186 has very high B values, > 100 Å$^2$ for Trp186 which is completely solvent-exposed, whereas in our structure, this loop is well determined with Trp186 well packed and well ordered (B = 30 Å$^2$). It was also necessary to reverse the directionality of the A chain from that in the R3 structure in order to fit the strong, well-defined density observed for several residues before, after, and including the disulfide that links the A chain to the B chain.

Many of the asparagine and glutamine sidechains in the R3 structure were re-oriented with respect to the flip of the sidechain amide; of these 18 sidechains, 16 are unambiguously orientable because of hydrogen bonds to neighboring residues. The two that are not orientable are mobile surface residues that do not make hydrogen bonds. Of the ten histidine sidechains, all are well determined, and nine have unambiguous orientations with respect to the flip of the imidazoles.

In the C2 uPA structures of this study determined from crystals grown in the presence of citrate, there are three citrate molecules at intermolecular regions including one near the active site. One acid group of the latter citrate occupies a region near the oxyanion hole, its carboxylate oxygens accepting a hydrogen bond from $N_{Gly193}$ and from $O\gamma_{Ser195}$. Another acid group makes a hydrogen-bonded salt bridge with $N\varepsilon2_{His57}$.

## Discussion

### Hydrogen-bonding differences between the S1 sites of Ser190 and Ala190 serine proteases that impart inhibitor selectivity

Most trypsin-like serine protease targets for drug design fall into three classes: those with serine, threonine or alanine at position 190. The S1 sites of the Ser190 and Ala190 sets of proteases, compared in this study, exhibit steric and electrostatic differences that can be exploited to engineer inhibitor selectivity. One factor contributing to the selectivity of 4-iodobenzo[*b*]thiophene-2-carboxamidine for uPA and against tPA is an additional hydrogen bond between the inhibitor amidine and $O\gamma_{Ser190}$ that is absent in the Ala190 proteases. This difference in hydrogen bonding at the S1 site is reflected in a marked trend of greater potency of each of the four amidine inhibitors for the Ser190 proteases than for the Ala190 counterparts (Table 1).

The more important component of the multi-centered N1–$O\gamma_{Ser190}$–water1 hydrogen-bonding network in the uPA– and trypsin–inhibitor complexes of this study is the N1–$O\gamma_{Ser190}$ interaction. In uPA– and trypsin–4-iodobenzo[*b*]thiophene-2-carboxamidine, pH 6.5 and

**Figure 4**

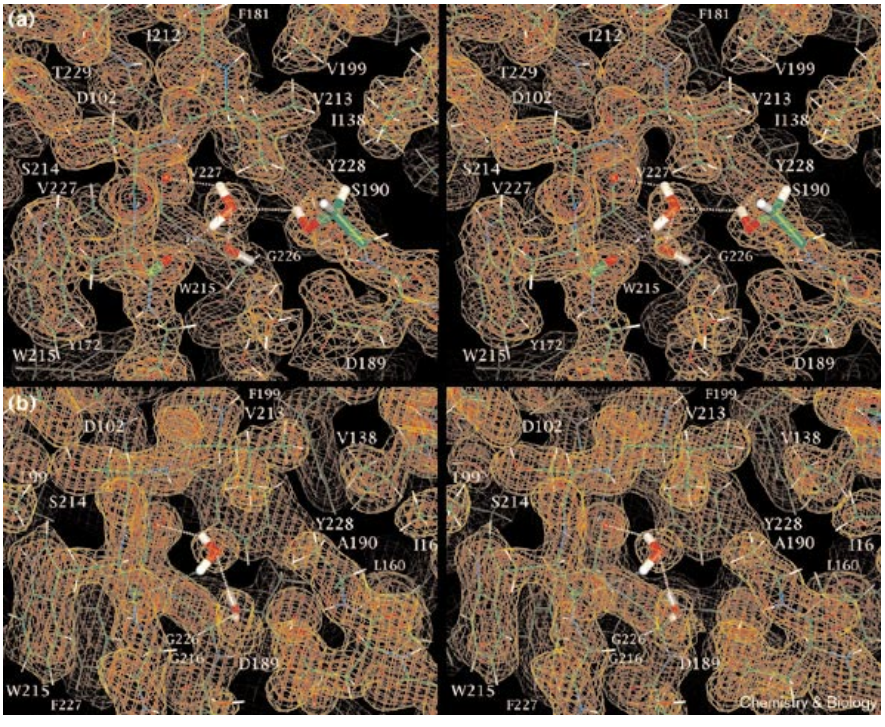


Structures and associated ($2|F_o|-|F_c|$), $\alpha_c$ maps for **(a)** apo-trypsin, pH 7.7; and **(b)** apo-thrombin, pH 7.5, 1.47 Å resolution. In (b), the long water1–$O_{Trp215}$ distance (3.4 Å) is indicated in cyan.

5.5, respectively, the N1–O$\gamma_{Ser190}$ length is shorter than the N1–water1 length by 0.5 and 0.7 Å, respectively (Table 2). To compensate for the absence of the N1–O$\gamma_{Ser190}$ hydrogen bond in thrombin–4-iodobenzo-[*b*]thiophene-2-carboxamidine, the N1–water1 hydrogen bond is shortened, by 0.3 Å, from the value in the corresponding uPA complex, and by 0.2 Å and 0.6 Å from the values in the trypsin complex at pH 5.5 and 8.2, respectively (Table 2). The N1–H1–water1 angle is nonoptimal, 130°, in both the uPA and thrombin complexes. The single nonoptimal hydrogen bond involving H1 in thrombin–4-iodobenzo[*b*]thiophene-2-carboxamidine is, therefore, expected to provide less binding affinity than the multi-centered hydrogen-bonding interactions in the corresponding uPA and trypsin complexes. The increase in free energy of binding of 4-iodobenzo[*b*]thiophene-2-carboxamidine in the Ser190 proteases, can be estimated from the ratios of the $K_i$ values in Table 1. The increase in free energy of binding of 4-iodobenzo[*b*]thiophene-2-carboxamidine in the Ser190 proteases can be estimated from the ratios of the $K_i$ values in Table 1 ($\Delta\Delta G_{binding}$ in kcal/mol for a pair of complexes with $K_i$ values of $K_i1$ and $K_i2 = 1.1335 \times \log(K_i1/K_i2)$). The increase ranges from 1.4 ± 0.1 kcal/mol (for the tryptase, tPA pair) to 2.9 ± 0.2 kcal/mol (for the uPA, factor Xa pair).

The decrease in the N1–water1 hydrogen bond length to 2.9 Å in the thrombin–4-iodobenzo[*b*]thiophene-2-carboxamidine complex from 3.2 Å in the uPA complex is associated with other changes unfavorable for inhibitor binding: a lengthening of the N1–O$\delta1_{Asp189}$ hydrogen bond from 2.8 to 3.1 Å, and a change in the thiophene–amidine dihedral angle from 11° to –1°. The greater planarity of the inhibitor in the thrombin complex is associated with an unfavorable contact between the thiophene hydrogen and an amidine hydrogen. The resulting increase in conformational energy of the thrombin-bound inhibitor from that of the uPA-bound inhibitor is estimated from *ab initio* calculations to be 0.5 kcal/mol.

A final factor favoring the binding of 4-iodobenzo[*b*]thiophene-2-carboxamidine to uPA over Ala190 counterparts involves the degree of order in the apo-enzymes of the water (water1) that mediates inhibitor binding. Because there is no hydrogen bond between water1 and the sidechain of residue 190 in the Ala190 proteases (Figure 4b), hydrogen-bond formation between water1 and the amidine inhibitors involves an increase in the order (and decrease in the entropy) of water1, reflected in a sizable decrease in its B-factor, by 15 Å$^2$, in the case of thrombin. In the inhibitor-free Ser190 counterparts, the position and orientation of water1 is more constrained by the hydrogen bond with O$\gamma_{Ser190}$ (Figure 4a), and thus less unfavorable entropy changes occur upon inhibitor binding; the decrease in its B factor is only 4 Å$^2$ in the case of trypsin.

### Other structural differences among the S1 sites of trypsin-like serine proteases that impart inhibitor selectivity

In addition to the direct influence of residue 190 on the structure and character of the S1 site, other longer-range forces exert indirect, but significant effects. For example, the rms mainchain positional difference, 0.35 Å, between a set of residues (at and near S1) of the superimposed S1 sites of uPA– and trypsin–4-iodobenzo[*b*]thiophene-2-carboxamidine (each having Ser190), is similar to the corresponding difference between the uPA (Ser190) and thrombin (Ala190) complexes (0.36 Å; Table 3a). These variations, determined by more global sequence differences (Table 3a), affect the relative locations, orientations and dihedral angles of bound inhibitors, and consequently the resulting hydrogen-bond lengths and van der Waals interactions between the protease and the inhibitor. The preference of small amidine inhibitors for Ser190 proteases over Ala190 counterparts observed in Table 1 is not, therefore, expected nor observed to be completely general.

### Diversity in the binding of small amidine inhibitors at the S1 sites of trypsin-like serine proteases

Within the set of protease–amidine complexes in this study, there are significant differences that involve the binding of a single inhibitor to different enzymes (Figure 2a–c, Table 3a), as well as the binding of different inhibitors to a single enzyme. These differences include the relative orientations of the bound inhibitors, their degree of planarity and their depths in the S1 pocket. There is a corresponding variability in the relative position and conformation of Asp189, and in the position and hydrogen-bonding interactions of the water co-bound at S1.

The structures of thrombin– and tPA–benzamidine [12] provide insight into the poor benzamidine potencies for these proteases ($K_i$ = 320 μM and 750 μM, respectively, Table 1). When bound to thrombin and tPA, benzamidine not only lacks a hydrogen bond with residue 190 (alanine in these cases), but also has considerable conformational strain (the phenyl-amidine dihedral is –7° in thrombin, and –3° in tPA).

An example of how structural features other than residue 190 can influence inhibitor affinity can be seen by comparing the structures and associated $K_i$ values for uPA– and trypsin–benzamidine, both of which have serine at position 190. The S1 site of uPA is deeper than that of trypsin; the O$\gamma_{Ser190}$–C$\alpha_{Ser195}$ distance is 0.5 Å shorter in trypsin–benzamidine than in uPA–benzamidine. The S1 site of uPA is also wider, by 0.7 Å, along the C$\alpha_{Asp189}$–N$_{Gly226}$ vector (Table S1a). These enlargements in the S1 pocket of uPA compared with that of trypsin result in the loss of the water1–O$_{Phe227}$ and water1–O$_{Trp215}$ hydrogen bonds in uPA–benzamidine compared with trypsin–benzamidine. The shift in the position of water1 in uPA–benzamidine, by 0.5 Å, from its location in

trypsin–benzamidine, is accompanied by an unfavorable change in the phenyl-amidine dihedral, from $-20 \pm 2°$ in trypsin–benzamidine, to 5° in uPA–benzamidine. The dihedral change corresponds to a calculated increase in conformational strain of 1.9 kcal/mol, larger than the actual decrease in binding energy of 0.9 kcal/mol calculated from the 4.6-fold decrease in affinity (Table 1). Favorable changes that may partially offset the conformational strain in uPA-bound benzamidine include the significantly shorter (by 3.3 σ and 5.0 σ, respectively) N1–$O\gamma_{Ser190}$ and water1–$O\gamma_{Ser190}$ hydrogen bonds (Table 2).

Comparison of the structures of the amidine complexes of uPA, tPA, trypsin and thrombin show, even with the simplest serine protease inhibitor (benzamidine), the important role of ordered solvent in mediating inhibitor binding, and the intricate partitioning of structural perturbations between changes in hydrogen bond lengths and in conformational strain. In Ser190 proteases, formation of the additional enzyme–inhibitor hydrogen bond involving Ser190 concurs with other interactions, including the $O\eta_{Tyr228}$–$O\gamma_{Ser190}$ and water1–$O\gamma_{Ser190}$ hydrogen bonds. These and other short- and long-range steric and electrostatic interactions at S1, determined from the local and global sequence, are often intricately coupled and cooperatively determine the structure and interactions of the bound inhibitor, its conformational strain and its affinity. The coupling renders the precise difference in the binding energy of the multi-centered ($O\gamma_{Ser190}$, water1, $N1_{inhibitor}$) hydrogen bond in Ser190 proteases versus the water1–N1 hydrogen bond in Ala190 proteases difficult to assess. Clearly, to determine and exploit the subtle structural differences at the S1 site that are important for inhibitor design requires high-resolution X-ray crystal structures of complexes involving both the target and the anti-target(s), even when their sequences are identical and their structures highly similar in the vicinity of inhibitor binding.

## Significance

**Involved or implicated in numerous disease states, trypsin-like serine proteases are rational, well-studied targets for therapeutic inhibition. Most of these targets and their anti-targets fall into three categories: those with threonine, serine or alanine residues at position 190. The ability to discriminate among these protease classes via small S1 recognition elements would provide a powerful basis for the design of small-molecule inhibitors that are both potent and specific for individual drug targets, such as urokinase-type plasminogen activator (uPA).**

**The $K_i$ values of 4-iodobenzo[*b*]thiophene-2-carboxamidine for uPA and for other trypsin-like serine proteases along with the structures of the associated complexes show that considerable specificity for uPA can be achieved through interactions at the S1 site alone. Although the S1 sites of uPA and tPA are highly similar to one another, they differ at position 190: alanine in tissue-type plasminogen activator (tPA), and serine in uPA. Ser190 is capable of making an additional hydrogen bond with S1-bound amidine inhibitors that can impart an increase in affinity of amidine inhibitors for uPA over Ala190 counterparts.**

**Comparison of the structures of the S1 sites of members of the Ala190 and Ser190 classes of trypsin-like serine proteases indicates that these sites are as different from one another within each class as they are between the two classes. Structural features in addition to the sidechain of residue 190 therefore differentiate the S1 sites of trypsin-like serine proteases and constitute a distinct fingerprint of each enzyme. Structural differences between S1 sites formed from identical segments of local sequence are imposed by the flanking sequence and structure. Specificity determinants at this site reside not only in its local structure but also in the degree and extent of its structural plasticity, determined by the sequence and structure of the neighboring regions. The depth, width, electrostatic character and spatial relationship of the S1 site to the active site and to other nearby binding sites such as S1′ constitute a unique signature of the target. When properly tuned to these parameters remarkably small inhibitors can attain considerable specificity.**

**Urokinase has emerged as a rational drug target for the treatment of breast and prostate cancer. The uPA–inhibitor complexes in this study are among the first small-molecule–uPA complexes reported, and are at resolutions significantly higher (1.7 Å) than the previously published uPA–peptide hemi-ketal structure (2.5 Å). Along with the related trypsin, thrombin and factor Xa structures described here they form part of a database that promises to expedite structure-based design of potent and specific small-molecule uPA inhibitors.**

## Materials and methods

*Preparation of deglycosylated low molecular weight human uPA*
*Cloning of LMW uPA.* The DNA fragment coding for LMW uPA was generated by polymerase chain reaction (PCR) amplification of pET-20HMUK, which contains the cDNA sequence of high molecular weight uPA (HMW uPA) cloned from a kidney cDNA population (Clontech, Palo Alto, CA). The amino terminus of our recombinant LMW uPA starts at residue 135 in the HMW uPA sequence. Amplification of LMW uPA was performed under standard conditions with a 5′ primer (5′-LMW-uPA = 5′-AAAAAACCGTCCTCTCCGCCGGAAGAAT-3′) coding for the amino acids KKPSSPPEE and a 3′ primer (3′-uPA-AvrII = 5′-CG**CCTAGG**TCAGAGGGCCAGGCCATTCTCTT-3′) containing an *Avr*II restriction site (bold). The PCR-amplified product was treated with Klenow fragment, digested with *Avr*II, and cloned into the *P. pastoris* expression vector pPIC9K (Invitrogen, San Diego, CA) linearized with *SnaB*I and *Avr*II. The sequence of LMW uPA in the expression construct (pPIC9KLMWuPA) was confirmed by sequencing.

*Construction of deglycosylated LMW uPA expression vector.* Deglycosylated LMW uPA (LMW uPA-N145A) has an Asn→Ala substi-

tution at position 302 in HMW uPA, or residue 145 of LMW uPA (chymotrypsin numbering scheme). The DNA fragment coding for LMW uPA-N145A was generated by amplifying upstream and downstream of the mutagenic site with primers, 5′-Ala-HindIII (5′-CC*AA**GCT**T*CTACCGACTATCTCTATCCGGAGCAGCT-3′) and 3′-Ala-*Hind*III (5′-CC*A-A**GCT**T*CTTTTCCAAAGCCAGTGATCTCACA-3′) coding for the Asn145→Ala substitution (bold type). Both mutagenic primers contain a new *Hind*III site (italicized) facilitating construction of the full-length DNA fragment coding for LMW uPA-N145A. The PCR-amplified LMW uPA(Ala145)-HindIII product (generated with 5′-LMW-uPA and 3′-Ala-HindIII primers) was treated with Klenow fragment and digested with *Hind*III. The HindIII-uPA(Ala156)-AvrII PCR product (generated with 5′-Ala-HindIII and 3′-uPA-AvrII primers) was digested with both *Hind*III and *Avr*II. The digested PCR fragments were then cloned into the *P. pastoris* expression vector pPIC9 (Invitrogen, San Diego, CA) linearized with *Sna*BI and *Avr*II. The sequence of the insert in the expression construct, pPIC9LMWuPA(N145A), was verified by sequencing.

*Transformation of* P. pastoris *and screening for expression of LMW uPA-N145A.* The pPIC9LMWuPA(N145A) expression construct was linearized with *Bgl*II, and used to transform the histidine-deficient *P. pastoris* strain GS115 by electroporation as described (*P. pastoris* expression kit instruction manual). Recombinant clones were cultured in buffered glycerol-complex (BMGY) medium and induced in buffered complex medium containing 0.5% methanol (BMMY). Cell-free culture supernatants were isolated, and the expression of recombinant enzyme was determined by silver-stained sodium dodecyl sulfate–polyacrylamide gel electrophoresis (SDS–PAGE) on a 12% acrylamide gel and by immunoblotting with a human uPA monoconal antibody (Oncogene Science). After activation with human plasmin, enzyme activity was assayed with the chromagenic substrate, Spectrozyme UK (American Diagnostica, Greenwich, CT).

*Purification of LMW uPA-N145A.* Purification of LMW uPA-N145A was based on affinity chromatography involving binding to p-aminobenzamidine [17]. Clarified *P. pastoris* supernatant was dialyzed into 20 mM MES (pH 6.0) with Amicon S1Y10 and passed through CM-Sepharose (Pharmacia). Urokinase in the gradient elution fractions was activated with plasmin at pH 8.5, 37°C for 2 h. The activated fractions were adjusted to pH 7.0 and made 1.0 M in NaCl before loading on a benzamidine-sepharose column (Pharmacia Biotech). Activated LMW uPA-N145A was eluted with 100 mM citric acid (pH 3.5), giving a single band on nonreduced SDS gel (data not shown).

*Synthesis of inhibitors.* Benzamidine was purchased from Sigma, and the starting materials and reagents for other compounds from Aldrich. 4-Iodobenzo[*b*]thiophene-2-carboxamidine and the corresponding noniodo analog, benzo[*b*]thiophene-2-carboxamidine were synthesized as described by Bridges *et al.* [18]. A similar procedure [19,20] was used to synthesize thieno[2,3-*b*]pyridine-2-carboxamidine (see Scheme 1 in the Supplementary material section). Synthetic details are described in the Supplementary material section.

*Enzymology*

Purchased enzymes were HMW uPA (American Diagnostica), tPA (Sigma), trypsin (Worthington), tryptase (Athens Research Technologies), thrombin (Calbiochem) and factor Xa (Haematological Technologies, Inc). The substrates for trypsin, tryptase, and thrombin (tosyl-Gly–Pro–Lys-p-nitroanilide), for factor Xa ($CH_3OCO$-D-CHA-Gly–Arg-pNA-AcOH, 'Pefachrome Xa') and one of the two substrates for HMW uPA (Bz-Ala–Gly–Arg-p-nitroanilide-AcOH, 'Pefachrome UK') were from Centerchem, Inc. The alternative substrate for HMW uPA (Cbz-L-(γ)Glu(α-t-BuO)-Gly-Arg-pNA, 'Spectrozyme UK') and the substrate for tPA ($CH_3$-$SO_2$-D-HHT-Gly–Arg-pNA, 'Spectrozyme tPA') were from American Diagostica Inc. Enzymes were assayed spectrophotometrically at ambient temperature in 50 mM Tris, 150 mM NaCl, 0.05% (v/v) Tween-20, 10% (v/v) DMSO, 0.002% antifoam, pH 7.4. The thrombin and factor Xa assays also contained 5.0 mM $CaCl_2$. The final concentrations of uPA, tPA, trypsin, factor Xa, tryptase and thrombin in the respective assays were 30, 11, 7.0, 3.0, 1.0 and 6.0 nM. The substrate concentrations of 100 μM (uPA), 200 μM (tPA), 100 μM (trypsin), 1000 μM (factor Xa), 500 μM (tryptase) and 250 μM (thrombin) were chosen based on the determined $K_m$ values of 85, 430, 100, 1000, 1620 and 280 μM, respectively. The rate of change in absorbance at 405 nm was measured immediately after addition of enzyme. Apparent inhibition constants ($K_i'$), were calculated by nonlinear least-squares regression analysis of the absorbance time course data using the software package BatchKi (developed and provided by Petr Kuzmic, Biokin Ltd., Madison, Wisconsin) using methodology similar to that described previously [21] for tight-binding inhibitors. These values were converted to $K_i$ values by the formula, $K_i = K_i'/(1 + S/K_m)$.

The $K_i$ values for inhibition of each enzyme by 4-iodobenzo[b]thiophene-2-carboxamidine were performed under assay conditions similar to those described above, except that concentrations of both the inhibitor and the substrate were varied (see the Supplementary material section), and the uPA substrate was Cbz-L-(γ)Glu(α-t-BuO)-Gly–Arg-pNA ('Spectrozyme UK') from American Diagnostica. Assay data were fitted to the equations describing competitive, noncompetitive and uncompetitive inhibition using the computer programs COMPO, NONCOMPO and UNCOMPO [22] and the $K_i$ values were obtained. The goodness of fit showed that inhibition was competitive.

*Crystallization and preparation of inhibitor-free proteases and of protease–inhibitor complexes*

*Human uPA complexes.* LMW human uPA-N145A was concentrated to 10 mg/ml using an Amicon Centricon-10 system and incubated in 50 mM HEPES, 5.0 mM NaCl, pH 7.4, 1.4 mM 4-iodobenzo[*b*]thiophene-2-carboxamidine for 15 min on ice. Potential crystallization conditions were screened in vapor diffusion drops with sparse matrix screening [23] kits purchased from Hampton Research, Laguna, CA. The complex was crystallized by vapor diffusion in hanging drops containing equal volumes of protein–inhibitor solution (0.28 mM LMW uPA-N145A, 1.4 mM inhibitor) and well solution (20% 2-propanol, 20% PEG 4K, 100 mM sodium citrate, pH 6.5) sealed over the well. Diamond plate crystals grew in 2 days. Other complexes were crystallized by a similar protocol at inhibitor concentrations at least tenfold higher than the $K_i$ values.

*Human thrombin–acetyl-hirudin and co-complexes.* Thrombin was purchased from Haematologic Technologies, Inc. and acetyl-hirudin from Bachem. Thrombin-acetyl-hirudin was prepared as described previously [24]. Thrombin (1.0 mg/ml in 50 mM HEPES, 50% glycerol, pH 7.0) was incubated with 1.0 mM acetyl-hirudin in the presence or absence of amidine inhibitors for 1 h at 4°C. The solution contained 5 equivalents of 4-iodobenzo[*b*]thiophene-2-carboxamidine, 10 mM benzamidine, or was saturated in [2,3-*b*]thienopyridine-2-carboxamidine (~2 mM). Glycerol was removed during concentration to ~10 mg/ml of the complexes with a centricon 10 (Amicon). Crystals of thrombin-acetyl-hirudin with or without co-bound small molecule inhibitors, pH 7.3 or 7.8, space group C2 (a = 71.2, b = 71.8, c = 72.7 Å, β = 100.7°) were grown in hanging drops by vapor diffusion after streak seeding. The structure without an inhibitor at the S1 site is referred to as apothrombin. The drops were made from 3 ml complex and 3 ml reservoir solution (0.10 M HEPES, 0.30 M NaCl, 22% (by volume) PEG 5K monomethyl ether, pH 7.5 or 8.2). Large single crystals of dimensions >0.2 mm in each dimension grew within 1 week.

*Bovine trypsin complexes and inhibitor-free trypsin.* Trypsin was crystallized as described previously [14]. A structure of $P3_121$ trypsin–benzamidine was determined at 1.20 Å resolution, in 2.02 M $MgSO_4$•7 $H_2O$, 100 mM MES, 1.0 mM $CaCl_2$, pH 7.5. The carboxamidine complexes were prepared by soaking trypsin–benzamidine crystals in synthetic mother liquor saturated in the inhibitors. The soaking solutions were replaced 4 times, about once a day. For the complexes determined at pH 8.2 the soaking solutions contained 1.73 M $MgSO_4$•7 $H_2O$, 150 mM Tris, 1 mM $CaCl_2$ and 2% dimethylsulfoxide (DMSO). For the 4-iodobenzo[*b*]thiophene-2-carboxamidine complex

**Table 4**

**Crystallography of urokinase, trypsin, and thrombin complexed with benzo[*b*]thiophene-2-carboxamidines, thieno[2,3-*b*]pyridine-2-carboxamidine, and benzamidine, and of apo-trypsin, apo-thrombin and apo-factor Xa.**

| RCSB PDB Code | 1C5X | 1C5N | 1C5R | 1C5Q | 1C5S | 1C5U | 1C5T |
|---|---|---|---|---|---|---|---|
| Protease | uPA | Thrombin | Trypsin | Trypsin | Trypsin | Trypsin | Trypsin |
| Inhibitor (APC #) | 6860 | 6860 | 6860 | 6860 | 7377 | 7538 | 7538 |
| pH | 6.50 | 7.33 | 5.50 | 8.20 | 8.20 | 5.50 | 8.20 |
| $R_{merge}$ (%)* | 8.8 | 6.3 | 9.1 | 8.7 | 5.0 | 9.0 | 5.7 |
| Resolution (Å) | 1.75 | 1.50 | 1.47 | 1.43 | 1.36 | 1.37 | 1.37 |
| Completeness (%) | 68 | 65 | 66 | 75 | 88 | 81 | 84 |
| $R_{cryst}$(%)† | 20.2 | 22.2 | 19.7 | 20.0 | 19.9 | 18.4 | 17.9 |
| Bond dev (Å)‡ | 0.017 | 0.018 | 0.019 | 0.018 | 0.019 | 0.020 | 0.018 |
| RCSB PDB Code | 1C5P | 1C5V | 1C5L | 1C5O | 1C5Z | 1C5Y | 1C5M |
| Protease | Trypsin | Trypsin | Thrombin | Thrombin | uPA | uPA | Factor Xa |
| inhibitor | Benzamidine | (apo) | (apo) | Benzamidine | Benzamidine | 7538 | (apo) |
| pH | 7.50 | 7.70 | 7.80 | 7.33 | 6.50 | 6.50 | 7.70 |
| $R_{merge}$ (%)* | 9.0 | 10.7 | 7.1 | 9.0 | 9.3 | 8.7 | 7.2 |
| Resolution (Å) | 1.21 | 1.48 | 1.47 | 1.90 | 1.85 | 1.65 | 1.95 |
| Completeness (%) | 88 | 61 | 69 | 51 | 64 | 68 | 60 |
| $R_{cryst}$(%)† | 19.4 | 20.0 | 21.7 | 20.3 | 18.9 | 20.3 | 22.6 |
| Bond dev (Å)‡ | 0.018 | 0.019 | 0.019 | 0.018 | 0.018 | 0.018 | 0.017 |

Inhibitors are coded as follows: APC-6860, 4-iodobenzo[*b*]thiophene-2-carboxamidine; APC-7377, benzo[*b*]thiophene-2-carboxamidine; APC-7538, thieno[2,3-*b*]pyridine-2-carboxamidine, . *$R_{merge} = \sum_h \sum_i |I(h)_i - \langle I(h)_i \rangle| / \sum_h \sum_i I(h)_i$. †$R_{cryst} = \sum(||F_o| - |F_c||)/\sum|F_o|$ (for reflections from 7.5 Å to the upper resolution). ‡rmsd values from ideal bond lengths.

at pH 5.5, the soaking solution was 85% saturated sodium citrate, 1 mM $CaCl_2$, 2.0% DMSO, saturated with inhibitor, pH 5.5. The pH was adjusted with saturated citric acid. For the thieno[2,3-*b*]pyridine-2-carboxamidine complex, pH 5.5, the soaking solution was 1.73 M $MgSO_4$•7 $H_2O$, 150 mM MES, 1 mM $CaCl_2$, 2% DMSO. To prepare inhibitor-free trypsin crystals, trypsin–benzamidine crystals were soaked at the target pH values for several weeks in 1.84 M $MgSO_4$•7 $H_2O$, 150 mM MES or Tris, 1.0 mM $CaCl_2$, during which the soaking solutions were periodically replaced.

*Factor Xa.* Lyophilized human factor Xa was purchased from Enzyme Research Laboratories Inc. The amino-terminal Gla-domain and carboxyl terminus were removed by incubation at 37°C with cathepsin G and carboxypeptidase B, and the truncated human factor Xa purified by high-performance liquid chromatography (HPLC) using a mono Q HR5/5 anion exchange column, as described previously [25]. Crystals of truncated human factor Xa (space group $P3_121$, a = b = 81.8 Å, c = 108.8 Å) were grown in hanging drops from equal volumes of protein solution (5.0 mg/ml in 20 mM HEPES, 50 mM $(NH_4)_2SO_4$, pH 8.0) and well solution (25% PEG 5K, 0.10 M Hepes, 0.2 M $(NH_4)_2SO_4$, pH 7.5). The drops were sealed over the wells. Crystals > 0.20 mm in each dimension grew after 2 weeks.

### *Crystallography*

Crystallographic data were collected with an R-AXIS IV image plate as described in [14] and in the Supplementary material section. For trypsin–benzamidine, pH 6.5, the crystal-to-detector distance was 76.0 mm, 2θ was 15.0°, and data were collected for 10 days during which the crystal underwent minor decay. The uPA and fXa structures were solved by molecular replacement by procedures similar to those described previously [26] (see the Supplementary material section) using the uPA and factor Xa structures (1lmw [13] and 1hcg [27]), respectively, obtained from the Brookhaven Databank [16]. Initial structures of trypsin and thrombin complexes were determined as described previously [14], the latter from the isomorphous structure, 1hag [28], in the Brookhaven Database. Structures were refined with X-PLOR and with difference Fourier analysis as described previously [14,26] (see the Supplementary material section). RCSB PDB codes, and data collection and refinement statistics, are given briefly in Table 4, and in more detail in Table S2.

*Superposition and comparison of structures.* For each pair-wise comparison, structures were initially superimposed based on sets of S1, S1′ and active site mainchain atoms summarized in Table 3. After inspection of the initially superimposed structures, residues were then excluded from the superpositions in order to maximize similarities and differences in the inhibitor-binding sites. Averages and standard deviations in hydrogen bond lengths and other parameters were calculated for uPA–4-iodobenzo[*b*]thiophene-2-carboxamidine (for which two structures were independently determined) and for trypsin–benzamidine (for which ten structures [14,29] in two crystal forms were independently determined at resolutions of better than 1.5 Å resolution in this and other published and unpublished studies. The comparisons of the two crystal forms of trypsin in the paper involve the $P2_12_12_1$ small-cell form (a = 54.8 Å, b = 58.7 Å, c = 67.6 Å) and the $P3_121$ form (a = 54.9 Å, c = 109.3 Å).

### Ab initio *calculations of amidine rotational barriers*

*Ab initio* calculations were performed on benzamidine and benzo[*b*]-thiophene-2-carboxamidine with Gaussian94 [30] by the Hartree-Fock method with the 6-31G* basis set. Geometry optimization with the Berny algorithm [31] used redundant internal coordinates. Calculations were carried out with no dihedral constraints or with dihedrals fixed at values of 0°, 3°, 10°, 17° and 30°. Energies were plotted as a function of dihedral angle to allow calculation of energy differences corresponding to any changes in dihedral angles.

*Accession numbers*

The atomic coordinates for these structures have been deposited with the Protein Data Bank with the following accession codes: 1C5X uPA–APC-6860; 1C5N, thrombin–APC-6860; 1C5R, trypsin–APC-6860; 1C5Q, trypsin–APC-6860;1C5S, trypsin–APC-7377; 1C5U, trypsin–APC-7538;1C5T, trypsin–APC-7538; 1C5P, trypsin–benzamidine; 1C5V, apo-trypsin; 1C5L, apo-thrombin ; 1C5O, thrombin–benzamidine; 1C5Z, uPA–benzamidine; 1C5Y, uPA–APC-7538; 1C5M, apo-factor Xa.

*Supplementary material*

Supplementary material including analysis of the discrete disorder of the inhibitor in the uPA–thieno[2,3-*b*]pyridine-2-carboxamidine complex, details of synthesis of the inhibitors, of enzymology, and of crystallography is available at http://current-biology.com/supmat/supmatin.htm.

## Acknowledgements

We thank Joanna Chmielewska, Tomas Lundqvist, Erifili Mosialou, and Derek Ogg (Pharmacia and Upjohn) for the modified factor Xa, and James Janc for help with the enzymology.

## References

1. Schechter, I. & Berger, A. (1967). On the size of the active site in proteinases. I. Papain. *Biochem. Biophys. Res. Commun.* **27**, 157-162.
2. Renatus, M., Bode, W., Huber, R., Stürzebecher, J. & Stubbs, M.T. (1998). Structural and functional analyses of benzamidine-based inhibitors in complex with trypsin: implications for the inhibition of factor Xa, tPA, and urokinase. *J. Med. Chem.* **41**, 5446-5456.
3. Maduskie, T.P. Jr., McNamura, K.J., Ru, Y., Knabb, R.M. & Stouten, P.F.W. (1998). Rational design and synthesis of novel, potent bis-phenylamidine carboxylate factor Xa inhibitors. *J. Med. Chem.* **41**, 53-62.
4. Gabriel, B., *et al.*, & Moroder, L. (1998). Structure-based design of benzamidine-type inhibitors of factor Xa. *J. Med. Chem.* **41**, 4240-4250.
5. Brandstetter, H., *et al.*, & Engh, R.A. (1996). X-ray structure of active site-inhibited clotting factor Xa: implications for drug design and substrate recognition. *J. Biol. Chem.* **271**, 29988-29992.
6. Towle, M.J., Lee, A., Maduakor, E.C., Schwartz, C.E., Bridges, A.J., Littlefield, B.A. (1993). Inhibition of urokinase by 4-substituted benzo[*b*]thiophene-2-carboxamidines: an important new class of selective synthetic urokinase inhibitor. *Cancer Res.* **53**, 2553-2559.
7. Dano, K., Andreasen, P.A., Grondahl-Hansen, J., Kristensen, P., Nielsen, L.S. & Shriver, L. (1985). Plasminogen activators, tissue degradation, and cancer. *Adv. Cancer Res.* **44**, 139-266.
8. Andreasen, P.A., Kjøller, L., Christensen, L. & Duffy, M.J. (1997). The urokinase-type plasminogen activator system in cancer metastasis: a review. *Int. J. Cancer* **72**, 1-22.
9. Rabbani, S.A. & Xing, R.H.M. (1998) Role of urokinase (uPA) and its receptor (uPAR) in invasion and metastasis of hormone-dependent malignancies. *Int. J. Oncol.* **12**, 911-920.
10. Stack, M.S., Ellerbroek, S.M. & Fishman, D.A. (1998). The role of proteolytic enzymes in the pathology of epithelial ovarian carcinoma. *Int. J. Oncol.* **12**, 569-576.
11. Magill, C., Katz, B.A. & Mackman, R. (1999). Emerging therapeutic targets in oncology: urokinase-type plasminogen activator system. *Emerging Therapeutic Targets* **3**, 109-133.
12. Lambda, D., *et al.*, & Bode, W. (1996). The 2.3 Å crystal structure of the catalytic domain of recombinant two-chain human tissue-type plasminogen activator. *J. Mol. Biol.* **258**, 117-135.
13. Spraggon, G., *et al.,* & Jones, E.Y. (1995). The crystal structure of the catalytic domain of human urokinase-type plaminogen activator. *Structure* **3**, 681-691.
14. Katz, B.A. & Luong, C. (1999). Recruiting $Zn^{+2}$ to mediate potent specific inhibition of serine proteases. *J. Mol. Biol.* **292**, 669-684.
15. Perrin, D.D. (1965). Dissociation constants of organic bases in aqueous solution. Supplement to Pure and Applied Chemistry, International Union of Pure and Applied Chemistry, London, Butterworths.
16. Bernstein, F.C., *et al.,* & Tasumi, M. (1977). The Protein Data Bank: a computer-based archival file for macromolecular structures. *J. Mol. Biol.* **112**, 535-542.
17. Holmberg, L., Bladh, B. & Astedt, B. (1976). Purification of urokinase by affinity chromatography. *Biochim. Biophys. Acta* **445**, 215-222.
18. Bridges, A., Littlefield, B.A. & Schwartz, C.E. *Urokinase Inhibitors.* 23 August 1994, US Patent 5340833.
19. Bhat, B. & Bhaduri, A.P. (1984) A Novel one-step synthesis of 2-methoxycarbonylthieno[2,3-*b*]quinolines and 3-hydroxy-2-methoxycarbonyl-2-3-dihydrothieno[2,3-*b*]-quinolines. *Synthesis* **8**, 673-676.
20. Meth-Cohn, O. & Narine, B. (1978). A versatile new synthesis of quinolines, thienopyridines and related fused pyridines. *Tetrahedron Lett.* **23**, 2045-2048.
21. Kuzmic, P. (1996). Program DYNAFIT for the analysis of enzyme kinetic data: application to HIV proteinase. *Anal. Biochem.* **237**, 260-273.
22. Cleland, W.W. (1979). Statistical analysis of enzyme kinetic data. *Methods Enzymol.* **63**, 103-138.
23. Jancarik, J. & Kim, S.H. (1991). Sparse matrix sampling: a screening method for crystallization of proteins. *J. Appl. Crystallogr.* **25**, 408-411.
24. Skrzpczak-Jankun, E., Carperos, V.E., Ravichandran, K.G., Tulinsky, A., Westbrook, M. & Maraganore, J.M. (1991). Structure of the hirugen and hirulog 1 complexes of α-thrombin. *J. Mol. Biol.* **221**, 1379-1393.
25. Chmielewska, J., Lundqvist, T., Mosialou, E. & Ogg, D. *Modified human factor Xa.* 7 February 1998, International patent WO 98/28412.
26. Katz, B.A., Liu, B., Barnes, M. & Springman, E.B. (1998). Crystal structure of recombinant human tissue kallikrein at 2.0 Å resolution. *Protein Sci.* **7**, 875-885.
27. Padmanabhan, K., *et al.,* & Kisiel, W. (1993). Structure of human des(1–45) factor Xa at 2.2 Å resolution. *J. Mol. Biol.* **232**, 947-966.
28. Vijayalakshmi, J., Padmanabhan, K.P., Mann, K.G. & Tulinsky, A. (1994). The isomorphous structures of prethrombin2, hirugen- and PPACK-thrombin: changes accompanying activation and exosite binding to thrombin. *Protein Sci.* **3**, 2254-2271.
29. Katz, B.A., Finer-Moore, J.S., Mortezaei, R., Rich, D.H. & Stroud, R.M. (1995). Novel $K_i$ ~ nanomolar inhibitors of serine proteases by binding or epitaxial chemistry on an enzyme surface. *Biochemistry* **34**, 8264-8280.
30. Frisch, M.J., et al., & Pople, J.A. (1995). *Gaussian 94, Revision E.3.* Gaussian, Inc., Pittsburgh PA.
31. Schlegel, H.B. (1982). Optimization of equilibrium geometries and transition structures. *J. Comp. Chem.* **3**, 214.